Carbon 139 (2018) 1063–1073

Contents lists available at ScienceDirect

Carbon

journal homepage: www.elsevier.com/locate/carbon

Flexible solar cells based on carbon nanomaterials

Xuemei Fu, Limin Xu, Jiaxin Li, Xuemei Sun*, Huisheng Peng**

State Key Laboratory of Molecular Engineering of Polymers, Department of Macromolecular Science and Laboratory of Advanced Materials, Fudan University, Shanghai, 200438, China

ARTICLE INFO

Article history:
Received 16 July 2018
Received in revised form
7 August 2018
Accepted 8 August 2018
Available online 9 August 2018

ABSTRACT

Flexible photovoltaic devices have attracted much attention because of the promising applications in portable or wearable electronics, power-generated textiles, building-integrated photovoltaic systems, electric automobiles, unmanned aerial vehicles and space robots. And due to the advantages of abundance, long-term stability, good transparency, high conductivity and mechanical flexibility, carbon nanomaterials have been widely used for realizing the flexibility and high performance of solar cells. In this review, the photovoltaic devices including dye-sensitized solar cells, organic solar cells and perovskite solar cells, which can be made flexible, are first introduced briefly. The necessity for carbon nanomaterials including fullerene, carbon nanotube and graphene is then summarized for the photovoltaic applications. The main efforts are next made to discuss the recent advances of the carbon nanomaterials for flexible solar cells with an emphasis on the material synthesis and structure design. The remaining challenges and future directions are finally concluded to guide the following studies on the development of carbon nanomaterials for flexible solar cells.

Contents

1. Introduction

Flexible solar cells have recently become a promising direction in photovoltaics as they are lightweight, endurable to complex deformations, integrated into curved surfaces, compatible to roll-to-roll manufacturing and convenient in storage and transportation [1–4]. Therefore, they hold out the prospect of application in portable or wearable electronics, power-generated textiles, building-integrated photovoltaic systems, electric automobiles, unmanned aerial vehicles and space robots [5–7]. Although amorphous silicon solar cells and the other thin-film photovoltaic devices have been made flexible, the poor bending radius and high

* Corresponding author.
** Corresponding author.
E-mail addresses: sunxm@fudan.edu.cn (X. Sun), penghs@fudan.edu.cn (H. Peng).

https://doi.org/10.1016/j.carbon.2018.08.017
0008-6223/

cost fall far short of what people expect [8]. To this end, new-type solar cells typically including dye-sensitized solar cells (DSCs) [9], organic solar cells (OSCs) [10] and perovskite solar cells (PSCs) [11], have been attractive reasonably for the low-temperature fabrications (below~150 °C), low thicknesses and tunable colors [12]. Generally, these solar cells are composed of three key parts, i.e., cathode, photoactive layer and anode. Moreover, electron transport layer (ETL) and hole transport layer (HTL) are introduced to reduce charge recombination in PSCs and OSCs, and electrolytes are required for charge transport and redox reaction in DSCs. For flexible solar cells, all the functional layers should be made flexible especially the electrodes, which also function as substrates for active layers. Besides, the interactions between the flexible electrodes and active layers *via* low-temperature processing are crucial to varying the morphology and interface for all the functional layers, thus influencing the performances of the photovoltaic devices [13,14].

Carbon nanomaterials, including fullerene, carbon nanotubes (CNTs) and graphene, have attracted broad interests at the energy community due to the promising advantages of high conductivity, mechanical flexibility, adjustable energy levels and long-term stability [15–19]. These high performances make them good candidates in flexible solar cells to be used as electrodes, charge transport materials or photoactive layers [20,21].

In this review, three kinds of solar cells that can be made flexible are first summarized. Three types of carbon nanomaterials mentioned above are then compared for the photovoltaic properties. We will focus on the main progress of flexible solar cells based on the carbon nanomaterials for high photovoltaic performances. It is finally highlighted to present the key challenges and future directions in the flexible solar cells using carbon nanomaterials.

Despite the numerous reports about flexible electronics not limited to solar cells both in academia and industry, it is rare to define the flexibility. We here try to make a definition on the flexibility for the future comparison on the mechanical property of the flexible electronic devices. Generally, the so-called flexible electronic devices have been mainly fabricated by making them on flexible substrates such as polymers, and they are typically bendable, twistable or even stretchable. Bendability is mostly recognized to assess the flexibility *via* an index of curvature radius. Based on the available reports, electronic devices that maintain 80% of initial properties under bending with curvature radii from 10 cm to 1 mm can be considered “flexible”. If the curvature radius could further decrease to 1 mm or even lower, they may be called “ultra-flexible”. In most cases, flexible photovoltaic devices mainly include DSCs, OSCs and PSCs that will be discussed below.

Since the breakthrough made by Grätzel et al., in 1991 [22], DSCs have inspired plenty of researches for their low cost, easy fabrication process and working under ambient light conditions [23–26]. As shown in Fig. 1a, DSCs are typically comprised of a photoanode (typically semiconductor of titanium dioxide (TiO_2)-, zinc oxide (ZnO)-, or stannic oxide (SnO_2)- modified conductive substrate), a photoactive dye (e.g., *cis*-bis(isothiocyanato) bis(2,2′-bipyridyl-4,4′-dicarboxylato)-ruthenium(II) bis-tetrabutylammonium (N719), *cis*-di(isothiocyanato)-bis(4,4′-dicarboxy-2,2′-bipyridine) ruthenium(II) (N3), 3-{6-{4-[bis(2′,4′-dihexyloxybiphenyl-4-yl) amino-]phenyl}-4,4-dihexyl-cyclopenta-[2,1-b:3,4-b′]dithiophene-2-yl}-2-cyanoacrylic acid (Y123)), an electrolyte containing I_3^-/I^- or Co^{2+}/Co^{3+} redox couple and a counter electrode (e.g., Pt and carbon materials) [27]. Typically, dye molecules on the photoanode inject excited electrons into the conduction band of the semiconductor in photoanode under illumination, followed by electron migration to the external circuit. The electrons from external circuit are then returned to redox electrolyte *via* counter electrode. The dye molecules are regenerated by capturing electrons from redox electrolyte to complete a cycle of energy conversion. For the mostly studied DSCs with the use of liquid electrolytes, it is difficult to make flexible devices due to the difficulty in sealing them stably.

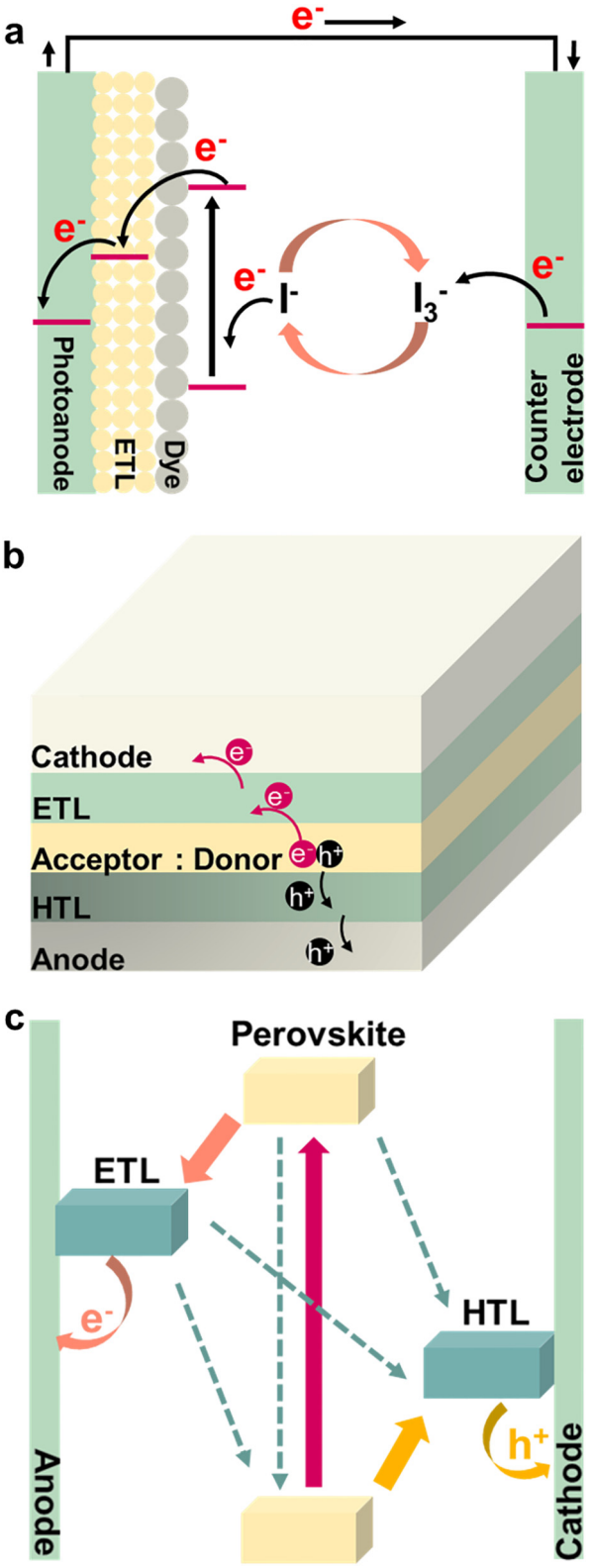

Fig. 1. Schematic diagrams to the device structure and work mechanism of (a) DSCs, (b) OSCs and (c) PSCs. (A colour version of this figure can be viewed online.)

Based on the all-solid-state advantage, OSCs have been more

explored for flexible solar cells [28,29]. For a typical structure in OSCs (Fig. 1b), an active layer comprising a p-type donor and a n-type acceptor like poly(3-hexylthiophene):phenyl-C_{61}-butyric acid methyl ester (P3HT:$PC_{61}BM$) is sandwiched between a cathode and an anode with two charge transport layers, namely ETL (e.g., TiO_2 and ZnO) between cathode and active layer and HTL (e.g., poly(3,4-ethylenedioxythiophene):poly(styrenesulfonate) (PEDOT:PSS)) between anode and active layer [30]. During the photoexcitation, electron-hole pairs also known as excitons are generated in electron donor of the active layer and then transferred to the interface between electron donor and acceptor, which are subsequently separated into electrons and holes. The electrons and holes are transported to the cathode and anode *via* ETL and HTL to generate voltage and current, respectively.

However, OSCs typically show relatively low power conversion efficiencies (PCEs). To this end, PSCs that show much higher PCEs up to 22.1% [31] also with all-solid-state nature and low-temperature processibility [32,33] have attracted increasing attentions in recent years. PSCs are also made by sandwiching photoactive perovskite layer between two charge transport layers (Fig. 1c), which adopt two categories of structures, namely, n-i-p junction for ETL/perovskite/HTL and p-i-n junction for HTL/perovskite/ETL [34]. For the photoactive layer of PSCs, perovskite refers to a class of compounds with the general structure of ABX_3, where A, B and X stand for monovalent cation (methylammonium ($CH_3NH_3^+$), formamidinium ($CH_2(NH_2)_2^+$), Cs^+, Rb^+), metal cation (Pb^{2+}, Sn^{2+}) and halide anion (I^-, Br^-), respectively [35]. After absorption of photons, electrons are excited from valence band of the perovskite to conduction band, leaving holes behind after separation of the weakly bound excitons. The electrons and holes are also transported though the ETL and HTL, followed by collection at the anode and cathode, respectively.

In order to fabricate flexible solar cells, a flexible front electrode atop which active materials are deposited should be firstly prepared. In other words, we need to replace the conventional rigid front electrode with flexible ones. Of course, the flexible front electrode should be transparent for the transmission of sun light. Note that if the back electrode is also transparent, a semi-transparent flexible solar cell can be obtained. To simultaneously realize the optical transparency and electrical conduction, transparent conductive oxides (TCO) are widely adopted due to the low sheet resistance at high transparency [30,36], e.g., 10–30 Ω/sq at >90% transparency for indium-doped tin oxide (ITO) electrode. TCO-modified polymer substrates are widely used as flexible front electrode, such as polyethylene terephthalate (PET)/ITO [33] and poly(ethylene naphthalate) (PEN)/ITO [37]. However, TCO suffers from intrinsic rigidness, brittleness and heaviness, which show limited flexibility even on polymer films [7]. Carbon nanomaterials may replace TCO due to their high conductivity, good transparency, high stability and flexibility [38,39], which will be detailed later.

Polymer substrates are unfavorable for the fabrication at high temperatures aiming at high efficiencies. For example, to reach high PCEs, the DSCs require the crystal transition of TiO_2 or the connection among TiO_2 nanoparticles at temperatures of 450–550 °C [40,41]. Similarly, high-temperature processed TiO_2 is required for high-performance PSCs [42]. To make better use of polymer substrates, low-temperature processed TiO_2 and other substitute materials including $PC_{61}BM$ and ZnO are developed but cause new obstacles [4,43]. To this end, free-standing metal substrates (e.g., Ti foil) are used [44,45]. However, these substrates are not flexible enough; they are not lightweight either, while a promising advantage of the flexible solar cells lies in the light weight. Therefore, free-standing electrodes based on metal wires are prepared for flexible fiber-shaped solar cells [46,47]. The design of thin photovoltaic fiber to reduce the electrode weight is more matching with the rising portable and wearable electronic products. Typically, two metal wires are twisted together with active materials between them to form a fiber-shaped solar cell. However, the lower effective contact area between two metal wires reduces its photovoltaic performance. Carbon nanomaterials like CNT and graphene are made into fiber and film electrodes for fiber-shaped solar cells that are bendable and twistable [48,49]. They can be further woven into flexible power textiles.

2. Carbon nanomaterials

Carbon nanomaterials show high conductivity, good transparency, high stability, good flexibility and adjustable energy levels, facilitating their applications in flexible solar cells. The corresponding structures and properties of carbon nanomaterials are concluded from zero-dimensional fullerene and one-dimensional CNT to two-dimensional graphene.

2.1. Fullerene

Fullerenes, discovered in 1895 [50], are stable and pure allotrope form of carbon. Spherically shaped fullerene is made of pentagons and hexagons in its structure. The well-known C_{60} fullerene consists of 12 pentagons and 20 hexagons with 60 bonds out of these 30 conjugated double bonds [51], and it shows high performances in thermal and pressure stabilities and chemical reactivity. C_{60} is fairly transparent and also has fair electrical conductivity (10^{-4} S/cm). Most importantly, C_{60} lacks bulky side-chains and can be packed more densely, which facilitates intermolecular charge transport. With good electron affinity, fullerenes represented by C_{60} and C_{70} and their derivatives are widely used as electron acceptors of photoactive layers in OSCs. Besides, they can also act as electron transport layers in PSCs due to the high carrier mobility at room temperature and appropriate energy levels.

However, early OSCs fabricated from conducting polymer/C_{60} bilayers, yielded low PCEs due to the poor solubility and miscibility and low lowest unoccupied molecular orbital (LUMO) of C_{60}. Thus, modified fullerenes with particular functional groups were employed to achieve better photovoltaic performances. Functionalized C_{60} with a phenyl and butyric acid methyl ester-containing side group, namely $PC_{61}BM$ (left of Fig. 2a) was prepared to improve the solubility [52]. Then it was found that the unsymmetrical $PC_{71}BM$ [53] (right of Fig. 2a) had even better solubility and optical absorption in the visible region compared with the symmetrical $PC_{61}BM$ [54]. C_{70} derivatives were also introduced into OSCs to improve photovoltaic performances. Besides, there were numerous investigations about the modifications of $PC_{61/71}BM$ concerning functional groups, such as aryl group, alkyl chain length and end group modification, aiming at the improvement of PCE. Also, the structure order of $PC_{61}BM$ could be optimized to enhance PCEs (Fig. 2b and c) [55].

2.2. Carbon nanotube

CNTs are representative one-dimension carbon nanomaterials. Since the discovery by Iijima in 1991 [56], CNTs have caused extensive researches both at academy and industry. CNTs can be regarded as hollow cylinders formed by winding single or multi-layered graphene sheets in different vector directions. Depending on the number of layers (n), CNTs can be classified into single-walled CNTs (SWCNTs) ($n = 1$), double-walled CNTs (DWCNTs) ($n = 2$) and multi-walled CNTs (MWCNTs) ($n \geq 3$) (Fig. 2d) [57]. CNTs typically have diameters of 0.7–20 nm and lengths ranged from nanometers to centimeters. SWCNTs can be uniquely described by the chiral vector, $\boldsymbol{C_h} = n\boldsymbol{a}_1 + m\boldsymbol{a}_2$, where $\boldsymbol{a_1}$ and $\boldsymbol{a_2}$ are

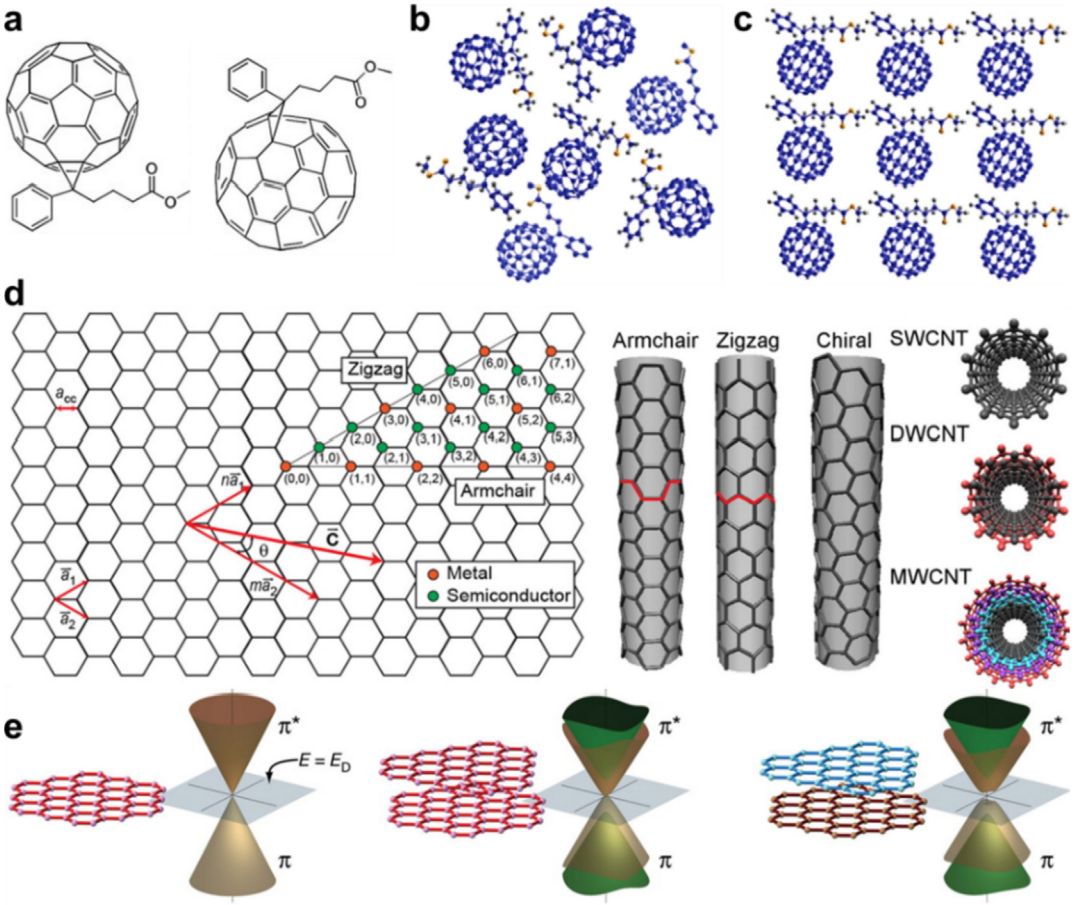

Fig. 2. (a) Structures of $PC_{61}BM$ (left) and $PC_{71}BM$ (right). Reprinted with permission from Ref. [53]. Copyright © 2016, John Wiley and Sons. (b, c) Schematic illustrations to the disordered and ordered $PC_{61}BM$ structures, respectively. Reprinted with permission from Ref. [55]. Copyright © 2016, Springer Nature. (d) Structures of CNTs. Reprinted with permission from Ref. [57]. Copyright © 2016 American Chemical Society. (e) Electronic structures of graphene in single, symmetrically double and unsymmetrically double layer forms. Reprinted with permission from Ref. [66]. Copyright © 2006, American Association for the Advancement of Science. (A colour version of this figure can be viewed online.)

unit cell vectors of the graphene lattice and n and m are integers. According to the rolling angles, SWCNTs can be classified into zigzag ($m = 0$), armchair ($m = n$) and chiral (other cases). The electronic properties of SWCNTs heavily depend on their chiral vectors. SWCNTs can be either metallic ($m = n$ or m-n is a multiple of 3) or semiconducting (all the other cases).

For solar cell applications, many important properties of CNTs have been well studied. Individual CNT has high intrinsic mobility exceeding 10^5 $cm^2/(V{\cdot}s)$ at room temperature and high electrical conductivity up to 10^6 S/cm [58–60], which is important for electrode materials. The Young's modulus, tensile strength and elongation at breaking of CNTs can reach 1–2 TPa, 10–100 GPa and 6–12% [61], respectively. In addition, the hollow tubular structures bring CNTs with high specific surface areas such as 1600 m^2/g [62] and low mass density. Also, it has a great thermal conductivity up to 3500 W/(m·K) [63]. These excellent properties provide a solid foundation for their applications in solar cells, such as the transparent front electrodes for OSCs and PSCs and counter electrodes for DSCs. CNTs can also be used as electron transport materials in DSCs and hole transport materials in PSCs, due to the high mobility and appropriate energy level. Besides, semiconducting SWCNTs can replace fullerene as electron acceptor in the active layer of OSC.

2.3. Graphene

As a representative two-dimensional carbon nanomaterial, graphene was discovered by Novoselov and coworkers with a micromechanical exfoliation method in 2004 [64]. It is a single-atom layer of sp^2-hybridized carbon arranged with a honeycomb structure. In a typical structure of graphene, each carbon atom is connected with three adjacent carbon atoms by σ bonds, and the p orbital electrons of all the carbon atoms are arranged side by side to form a delocalized conjugated large π bond. A theoretical thickness of graphene is 0.335 nm [65]. Graphene can be usually prepared and investigated in single layer, double layers and thicker films [66] (Fig. 2e).

Graphene shows many extraordinary properties suitable for application in flexible solar cell. Pristine graphene is reported to have intrinsic room-temperature electron mobility as high as 2×10^5 $cm^2/(V{\cdot}s)$ [65], electrical conductivity up to 10^4 S/cm and room-temperature thermal conductivity of ~5000 W/(m·K) [67], higher than that of SWCNTs (3500 W/(m·K)) and 12 times that of copper (400 W/(m·K)). Graphene also has excellent optical properties with a light transmittance of 97.7% and independent of the wavelength, so it is a perfect transparent electrode material instead of ITO [68]. Furthermore, graphene shows good mechanical properties, with strength and modulus of 125 GPa and ~1100 GPa, respectively. Graphene is also an ultra-light material with an areal density of only 0.77 mg/m^2, and it has a specific surface area of 2630 m^2/g [69]. Similar to CNTs, graphene with high electrical conductivity and transparency is regarded as an alternative to TCO in the field of flexible solar cells. Graphene was also reported for the

use in the photoanode of DSCs to improve electron transport and as electron acceptor to replace fullerene in OSCs. In addition, graphene can replace the noble metal catalyst as the counter electrode of DSCs.

3. Flexible solar cells based on carbon nanomaterials

3.1. Flexible dye-sensitized solar cells based on carbon nanomaterials

In flexible DSCs, fullerenes are rarely used, CNTs and graphene are mostly used in both fiber and planar forms. Flexible especially fiber-shaped DSCs are fabricated with CNTs commonly adopted as a substitute for Pt counter electrode, enabling reduction catalysis of the ions in the electrolyte to achieve rapid electron transport. Pan et al. discovered the aligned CNT fibers had a better catalytic activity for the thiolate/disulfide redox couple than traditional Pt counter electrode [70]. The flexible fiber-shaped DSCs based on CNT fibers achieved a maximal PCE of 7.33% while only a maximal efficiency of 2.06% was obtained using traditional Pt counter electrode.

Flexible DSCs based on I_3^-/I^- redox electrolyte are also developed using CNTs. Nevertheless, pristine CNTs present a lower catalytic performance than Pt for I_3^- reduction in DSCs. Hybridization or compositing with other active materials prove to be effective solutions. CNT hybrid fibers were prepared with CoSe nanoparticles decorated in CNT fiber *via* a simple hydrothermal treatment [71]. Depositing the active materials on CNT fibers could generate new catalytic sites, greatly enhancing the electrocatalytic activity of counter electrode in fiber-shaped DSCs. Thus, a PCE of 6.42% for modified fibers was achieved, higher than 3.4% and 5.6% for pristine CNT fibers and Pt wires, respectively. Then, Jiang et al. prepared Pt-modified aligned CNT fibers via an electrochemical deposition method [72]. The fiber-shaped DSC with the composited fiber as counter electrode achieved a much higher PCE of 8.10% compared with that of 4.91% for a bare CNT fiber. Surface modification is also an effective strategy for improving catalytic activity. The pristine hydrophobic CNT fibers were treated with an oxygen microwave plasma to introduce active defect sites and oxygen-containing functional groups on the surface, which also increased the hydrophilicity largely [73]. This plasma processing could improve the catalytic activity of CNTs and help for depositing Pt nanoparticles [74]. Fu et al. reported a fiber-shaped DSC with a record PCE of 10.00%, which outperformed all the other fiber-shaped solar cells [74]. A novel core-sheath CNT fiber was designed by asymmetrically twisting an aligned CNT sheets with hydrophobic and hydrophilic CNTs at two sides. Then the Pt-modified core-sheath CNT fiber was twined with a dye-absorbed Ti/TiO_2 wire, followed by redox electrolyte injection to fabricate the fiber-shaped DSC (Fig. 3a). Besides, the PCE did not show much decline under bending with increasing bending angles from 0 to 180° (Fig. 3b). Importantly, the fiber-shaped DSCs could be easily woven into textile also with high flexibility (Fig. 3c). Further, flexible fiber-shaped DSCs with stretchable ability were realized via novel elastic conducting CNT fiber electrodes [75]. The resulting fiber-shaped DSCs exhibited a PCE up to 7.13% that could be also well maintained under stretching.

Flexible DSCs using CNTs in photoanode have also been reported. Brittleness of TiO_2 materials is also one of barriers to realize flexible devices. Hence, Chen et al. reported a flexible DSCs with bare CNT fiber as photoanode followed by absorbing N719 dye on PEN/ITO flexible substrate [76]. Interestingly, the PCEs of the flexible DSCs slightly increased when bent up or down. Further, a flexible photoanode including TiO_2 particles and metallic or semiconducting SWCNTs was prepared on the PET/ITO [77]. Compared with semiconducting SWCNTs, metallic SWCNTs provided a greater PCE because of more efficient electron transport. Moreover, the mechanical network among TiO_2 particles constructed by metallic SWCNTs effectively provided flexibility and durability with only a small decrease in PCE when the entire cell was bent under a radius of 5 mm. The efficiency loss was primarily originated from ITO layer cracking. Then a robust device based on a Ti foil using metallic SWCNTs/TiO_2 photoanode was thus prepared to realize better flexibility, and no decrease in PCE occurred even after 1000 bending cycles, demonstrating high flexibility and durability. Moreover, fiber-shaped DSCs were also reported by using CNT fiber as both counter electrode and photoanode, thus exhibiting excellent flexible and stability [41].

In flexible DSCs, graphene is also mainly used to replace traditional Pt counter electrode. A highly conductive graphene-coated cotton fabric (HC-GCF) with a sheet resistance of only 7 Ω/sq was utilized as an efficient counter electrode in DSCs [78]. It presented an excellent electrocatalytic activity for reducing I_3^- and a negligible change of resistance at various bending angles. Moreover, it had an ideal tolerance to electrolyte solution and water washing. A high PCE of 6.93% was achieved with HC-GCF as counter electrode using polymer electrolyte. Actually, pristine graphene with a perfect structure may have a limited catalytic ability for the reduction reaction, since its electrocatalytic activity is usually related to the defects and edge positions. Therefore, some structural modifications are often required for graphene. Methods reported in the literature mainly include heteroatom doping [79] and compositing with metal sulfides [80] and conducting polymers [81]. For example, flexible DSCs based on nano-TiC/graphene/PEDOT:PSS composites as counter electrode on plastic substrate by spray printing were reported. The device achieved a PCE of 4.5%, slightly higher than that of a similar device using Pt counter electrode (PCE = 4.3%) [81].

Flexible DSCs were also fabricated based on graphene in a fiber form. Here, graphene was spun into a fiber, exhibiting a density of 0.61 g/cm^3, strengths of 10^2~10^3 MPa and electrical conductivities of 10^2~10^3 S/cm. Then it was modified with Pt nanoparticles to serve as the counter electrode of flexible fiber-shaped DSCs (Fig. 3d) [82]. The good mechanical strength, electrical conductivity and catalytic activity of graphene composite fibers resulted in a certified maximum PCE of 8.45% for the fiber-shaped DSCs in 2013.

In addition, graphene can also be added into the photoanode of DSCs, facilitating electron transport. Huang et al. fabricated a highly flexible DSC at room temperature, employing three-dimensional (3D) graphene decorated nanocrystalline TiO_2 film (3DGT) as photoanode on plastic substrate (Fig. 3e) [83]. Due to the enhanced charge transport and increased surface area from 3D conductive graphene skeleton, flexible DSCs based on the 13 μm-thick 3DGT-0.85 (0.85 wt% 3D graphene plus TiO_2 nanoparticles) photoanode achieved a PCE of 6.41% which was 56% higher than those based on bare TiO_2 photoanode.

3.2. Flexible organic solar cells based on carbon nanomaterials

For high-performance OSCs, efficient exciton dissociation is crucial, which requires an electron acceptor with high electron affinity and fair electrical conductivity. Fullerenes and their derivatives possess adjustable energy levels and high electron affinity, thus are popularly developed as the electron acceptor of flexible OSCs. Yu et al. reported a flexible planar OSC with P3HT: $PC_{61}BM$ as photoactive layer based on Ag nanowires and polymethacrylate composite electrode. The resulting device reached a PCE of 3.28% in 2011 [84]. This value was comparable to the PCE of 3.34% for control device on glass/ITO substrate. Besides, there were also some $PC_{71}BM$-based flexible OSCs explored, focusing on the corresponding donor materials, interface materials or fabrication

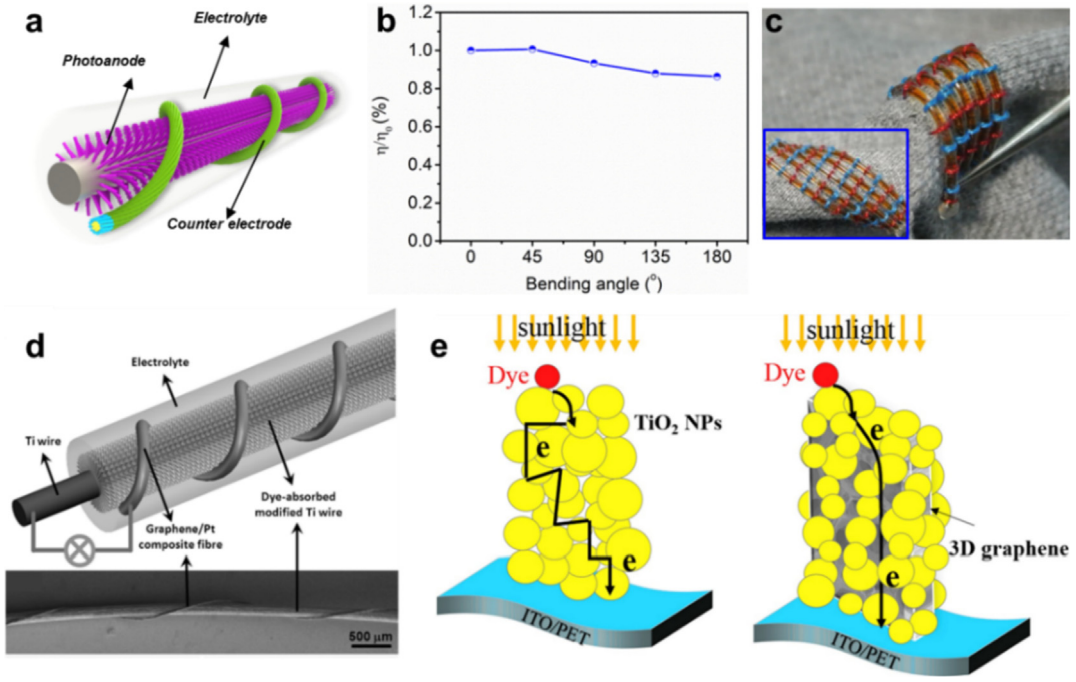

Fig. 3. (a) Schematic illustration to the flexible fiber-shaped DSCs based on CNT composite fibers. (b) The dependence of PCE on bending angle. (c) Photovoltaic textile based on the fiber-shaped DSCs. (a–c) Reproduced from Ref. [74] with permission from The Royal Society of Chemistry. (d) Schematic illustration and scanning electron microscope image of a DSC wire prepared using a graphene/Pt composite fiber as the counter electrode. Reprinted with permission from Ref. [82]. Copyright © 2013, John Wiley and Sons. (e) Schematic illustrations to the photoanodes of the flexible planar DSCs and electron transport path without (left) and with (right) 3D graphene network. Reprinted with permission from Ref. [83]. Copyright © 2015 Elsevier B.V. All rights reserved. (A colour version of this figure can be viewed online.)

process, together with the effect of bending on the device PCE. For instance, flexible OSCs (Fig. 4a and b) were attached conformably to the cylinders with radii of 7 and 4 mm [85]. It could be observed that, as expected, the PCE was slightly decreased after bending at a radius of 4 mm; interestingly, it became even higher after bending at a radius of 7 mm because of the improved functional layers with a photo-annealing process (Fig. 4c). Fullerenes and their derivatives were further introduced as ETL for OSCs. For instance, n-type self-doping fullerene electrolyte with [6,6]-Phenyl-C_{60} as the backbone was used as ETL in the inverted OSCs with PTB7-Th:$PC_{71}BM$ as photoactive layer [86]. The resulting device demonstrated an enhanced PCE of 10.04% in the flexible film.

Flexible planar OSCs can be fabricated with CNTs usually as electrodes which should be transparent and conducting to replace TCO. For instance, a flexible OSC was reported with metallic SWCNT-based transparent front electrode thermally doped by molybdenum trioxide (MoO_3), showing a higher transmittance than bare SWCNT films [87]. Moreover, the doped SWCNT film acted as a transparent electrode with electron-blocking function. The device on PET showed an efficiency of 3.91% and somewhat flexibility. Other doping methods were also developed. For comparison, aerosol SWCNT were p-doped by nitric acid doping via "sandwich transfer" and MoOx thermal doping via "bridge transfer" [88]. The resulting devices yielded PCEs of 4.1% and 3.4% based on the above two methods, respectively. Apart from doping, composite materials were also adopted. Conducting polymer modified CNTs, to be exact, PANI/CNT interfacial thin films were prepared, exhibiting an optical transmittance of 89% at 550 nm and a sheet resistance of 295 Ω/sq [89]. As a result, the flexible devices using the composite film on PET substrate presented a PCE of 2.27%.

By the way, semiconducting SWCNTs were also developed as electron acceptor to replace fullerene in OSCs [90], aiming for convenient synthesis, and better optical absorption and stability. However, the resulted device showed quite low PCE, owing to severe carrier recombination, and no flexible counterparts were reported.

Recently, flexible fiber-shaped OSCs were also developed with $PC_{61}BM$ as the electron acceptor and CNT fiber as electrode [91]. It showed good flexibility and maintained ~85% of its initial PCE after bending for 1000 cycles (Fig. 4d and e). These fiber-shaped OSCs could be further woven into desired OSC textiles without sacrificing flexibility obviously (Fig. 4f). Moreover, a stretchable fiber-shaped OSC was successfully fabricated by winding an aligned CNT sheet onto a spring-like electrode inserted with an elastic fiber [92]. Such OSC fibers exhibited a reasonable PCE, which was varied less than 10% after bending for 1000 cycles or under stretching at a strain up to 30%.

Flexible OSCs can also be obtained using graphene. Gradečak demonstrated graphene anode- or cathode-based flexible OSCs with PCEs of 6.1 or 7.1%, respectively [93]. The high PCEs were achieved via thermal treatment of MoO_3 electron blocking layer for graphene anode or direct deposition of ZnO ETL on graphene cathode. Graphene was also applied as both the anode and cathode to fabricate flexible and semitransparent OSCs via a new room-temperature dry-transfer technique [94]. An optical transmittance as high as 61% over the visible spectrum and PCEs of (2.8–4.1)% were achieved, by combining the transparent electrodes with photoactive organic compounds which absorbed light mainly in the ultraviolet and near-infrared regimes. Another semitransparent and flexible OSCs were fabricated from doped graphene layers, ZnO, P3HT:PCBM, and PEDOT:PSS as anode/cathode transparent electrodes, ETL, photoactive layer and HTL, respectively (Fig. 4g) [95]. For the transparent anode and cathode, graphene was doped with bis(trifluoromethanesulfonyl)-amide (TFSA) and triethylene tetramine (TETA), respectively. A PCE of 3.12% was achieved (Fig. 4h), which was further enhanced to 4.23% in virtue of an Al reflective mirror. It also presented high mechanical flexibility according to bending tests at various curvature radii (Fig. 4i).

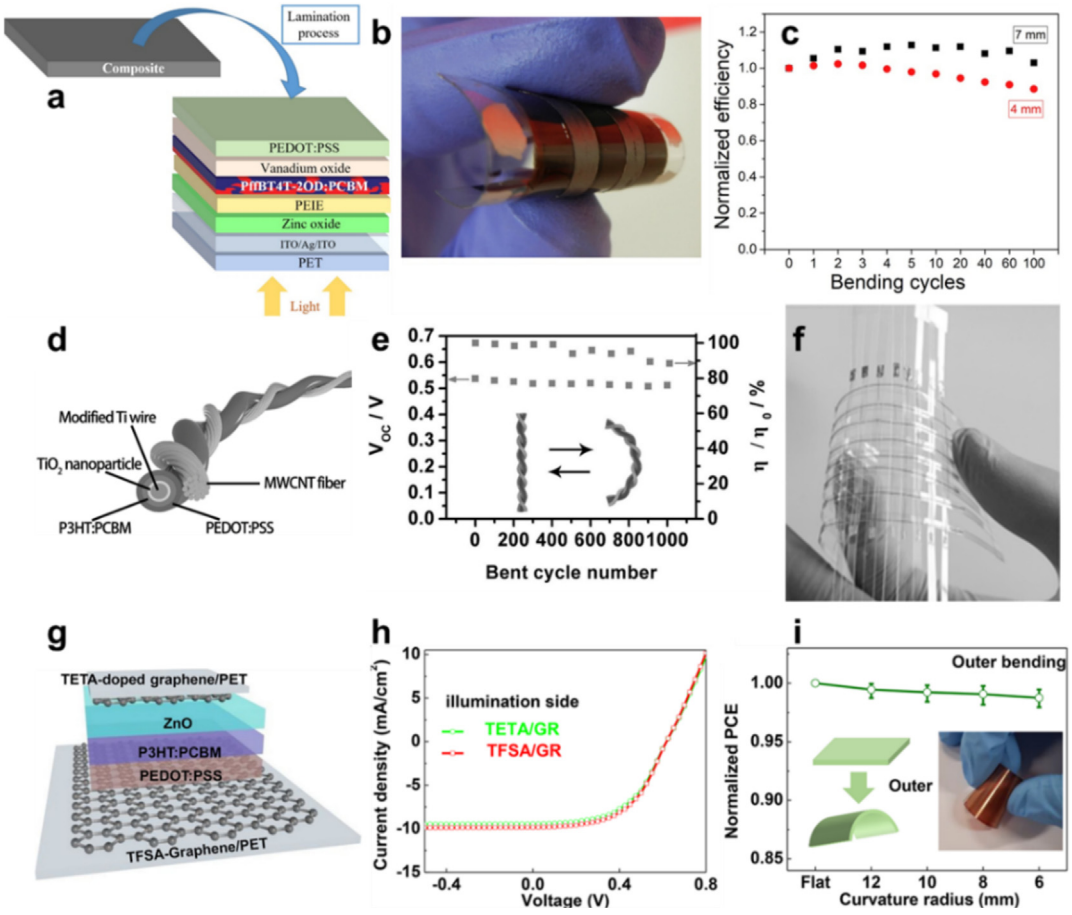

Fig. 4. (a–c) The flexible OSC with $PC_{71}BM$ as electron acceptor. (a) Schematic to the structure. (b) Photograph of the OSC under bending. (c) Bending cycle test. Reprinted with permission from Ref. [85]. Copyright © 2018 Elsevier Ltd. All rights reserved. (d–f) The fiber-shaped OSCs with $PC_{61}BM$ as electron acceptor and CNT fiber as anode. (d) Schematic to the structure. (e) Bending cycle test. (f) Photograph of the flexible energy textile woven from the fiber-shaped OSCs. Reprinted with permission from Ref. [91]. Copyright © 2014, John Wiley and Sons. (g–i) A flexible OSC with graphene as electrodes with the structure (g), *J-V* curves by illumination from TETA/GR and TFSA/GR electrode sides (h), and different bending radius test (i). The inserted schematic and photograph describe the bending test and a device under bending, respectively. Reprinted with permission from Ref. [95]. Copyright © 2017 American Chemical Society. (A colour version of this figure can be viewed online.)

3.3. *Flexible perovskite solar cells based on carbon nanomaterials*

Flexible PSCs can realize better stability at ambient conditions and low-temperature solution processing easily using fullerenes and their derivatives as ETL. For example, with a device structure of PET/ITO/PEDOT:PSS/Perovskite/$PC_{61}BM$/TiO_X/Al, a flexible PSC was fabricated at low temperature and could bear mechanical bending up to 20 times. The flexible device yielded a PCE of 6.4% [96] which was increased to 9.2% [42] after optimization. Compared with glass/ITO based counterparts with PCE of 11.5%, the lower PCE of PET/ITO based flexible devices might be ascribed to higher series resistance which could result in decreased short-circuit current density (J_{SC}) and fill factor (FF) [42]. To achieve a higher PCE, updated structure of PET/Ag-mesh/PH1000/PEDOT:PSS/perovskite/$PC_{61}BM$/Al for flexible PSCs were fabricated with a PCE of 14.2% (Fig. 5a and b) [1]. And the PCE showed almost no decrease even at 2 mm of bending radius, retaining 98.1% of the original value (Fig. 5c).

The PCEs and mechanical properties of flexible PSCs can be further improved by optimizing film morphology and composition of $PC_{61}BM$. For instance, poly([*N*,*N*′-bis(2-octyldodecyl)-1,4,5,8-naphthalene bis (dicarboximide)-2,6-diyl]-*alt*-5,5′-(2,2′-bithiophene)) (PNDI-2T) was incorporated into $PC_{61}BM$, which yielded electrical properties comparable to pure $PC_{61}BM$ but with enhanced mechanical stability [97]. It was resulted from the dispersion of $PC_{61}BM$ domains in the entangled polymeric PNDI-2T matrix, allowing electrons to pass through each domain and relieving mechanical stress on the $PC_{61}BM$ domains. Another low-temperature solution-processed material, pillar [5]arene-based small molecule material, termed C3, was incorporated between $PC_{61}BM$ and electrode to function as a single-layer buffer part [98]. The introduction of C3 enhanced the interface contact and reduced the interface barriers, which usually existed between $PC_{61}BM$ and electrode. It was also found that the C3 capping layer could improve the surface quality of $PC_{61}BM$, forming a smooth, dense and pinhole-free morphology with fewer surface defects. Thus, a device with PCE of 13.27% could be obtained based on PEN/ITO substrate.

Besides improving interfacial property, an alternative way to improve PCE is introducing another electron transport material to form double-layer ETL with $PC_{61}BM$. Ryu et al. synthesized nanocrystalline Ti-based metal-organic framework (nTi-MOF) particles with favorable property for charge injection and transport from perovskite to the electrode [99]. The combination of $PC_{61}BM$ with nTi-MOF ETL provided efficient electron transport and also suppressed direct contact between perovskite and the electrode. This resulted in a PCE of 17.43% for flexible PSCs. Using double fullerene layers composed of $PC_{61}BM$ and C_{60} as ETL, flexible PSCs with a record PCE of 18.1% were obtained by a low-temperature solution process [14]. The high PCE was resulted from the improved film morphology and composition via changing the precursor ratio of perovskite on PET/ITO substrate.

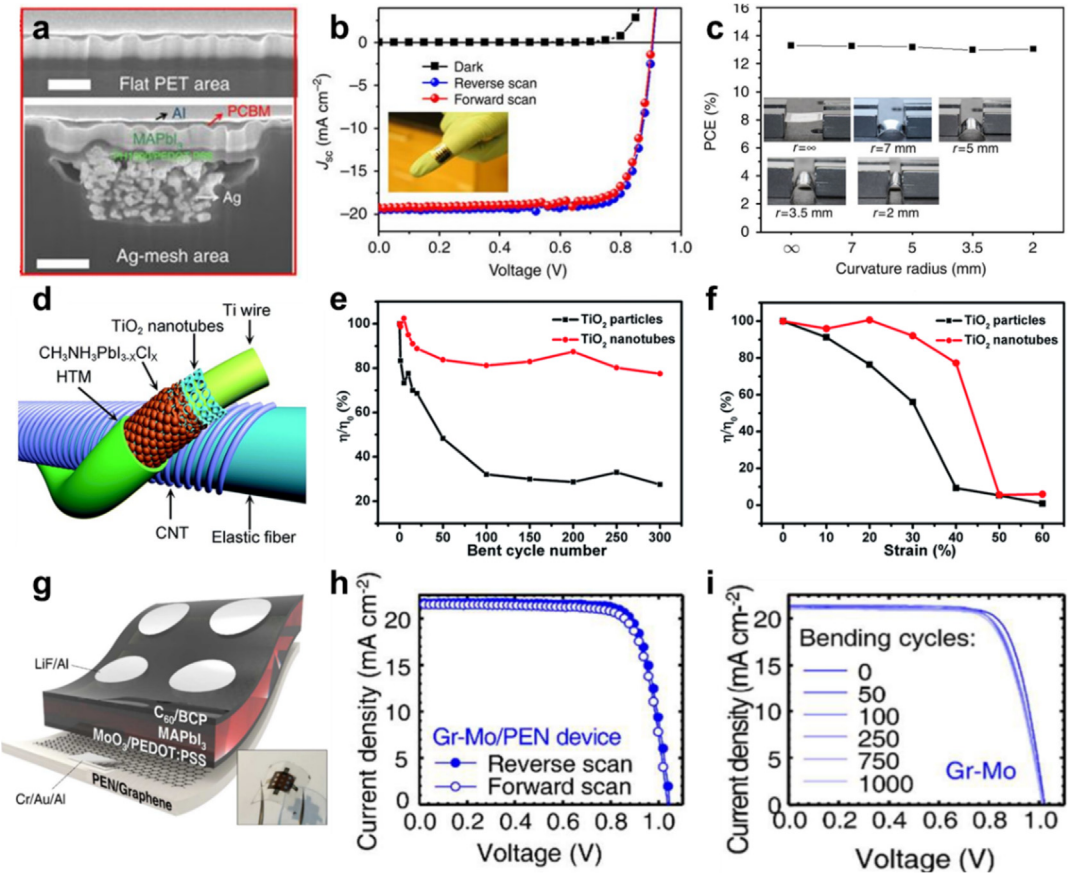

Fig. 5. (a–c) Structure, photovoltaic performance, and different bending radius test of flexible $PC_{61}BM$-based PSC, respectively. Adapted with permission from Ref. [1]. Copyright (2016) Springer Nature. (d–f) Structure of an elastic fiber-shaped PSC based on CNT (d) and the dependence of PCEs on the bending cycle (e) and stretching strain (f). Reproduced from Ref. [101] with permission from The Royal Society of Chemistry. (g–i) Structure, *J-V* curves and bending stability of graphene-based flexible PSCs, respectively. Reproduced from Ref. [105] with permission from The Royal Society of Chemistry. (A colour version of this figure can be viewed online.)

Apart from C_{60} and its derivatives, C_{70} was also used as ETL in flexible PSCs. Interlayered between TiO_2 and perovskite material, the resulted TiO_2/C_{70} ETL showed good surface morphology, efficient electron extraction and high-quality perovskite film, which could be attributed to suitable nanosize and superior electronic property of C_{70} molecules. In comparison with pristine TiO_2-based PSC counterparts, the PCE was increased by 28% [100].

CNTs are usually used as transparent front electrode or hole transport layer in flexible PSCs. In 2014, transparent conductive CNT network was deposited on top of perovskite and served as hole collector and transparent electrode simultaneously, and the flexible PSC showed a PCE of 8.31% [45]. After 100 bending cycles, the device showed little performance deterioration with PCE decreased from 6.01% to 5.06%, demonstrating good flexibility. Also based on CNTs, the first fiber-shaped stretchable PSC was developed by designing a stretchable aligned CNT-based conducting fiber and spring-like modified Ti wire as two electrodes with perovskite coated on the modified Ti wire (Fig. 5d) [101]. The PCE could be maintained above 80% under bending for 300 cycles and above 90% at a stretching strain of 30%, respectively (Fig. 5e and f), exhibiting a stable photovoltaic performance under both bending and stretching. Later on, a more efficient one-dimensional PSC was fabricated with a flat interface which improved the coverage and crystal size of perovskite layer [102]. A continuous aligned CNT sheet was closely wrapped on the perovskite layer, functioning as an electrode and HTL. The PSCs showed a high PCE of 9.49% with photovoltaic performances stabilized under both bending and twisting. In addition to transparent front electrode, CNTs can also function as back electrode where vacuum processed metals are adopted typically.

Graphene performs better as an efficient and robust transparent front electrode in flexible PSCs. In 2016, Yan et al. fabricated an ultrathin and flexible PSC using transparent graphene electrode with a device structure of PET/graphene/P3HT/$CH_3NH_3PbI_3$/$PC_{71}BM$/Ag on 20 μm-thick PET substrate by low-temperature solution process [103]. The flexible devices showed a PCE of 11.5% with high durability and air stability. A clear contrast was made by fabricating flexible, indium-free inverted PSCs where ITO was replaced with SWCNT or graphene [104]. The SWCNT- or graphene-based PSCs showed efficiencies of 12.8% and 14.2%, respectively. However, the SWCNT-based flexible PSCs showed a slightly higher mechanical stability than the graphene-based ones due to the entangled configuration of SWCNT network together with its inherent defect-free nature. Further endeavor utilizing chemical vapor deposition-grown graphene in single-layer form as a transparent electrode was reported by Choi and co-workers (Fig. 5g) [105]. A few-nanometer-thick MoO_3 layer was deposited to induce hole doping in graphene. The flexible devices achieved a high PCE of 16.8% (Fig. 5h) and a remarkable bending stability with the current density-voltage (*J-V*) curves remaining almost unchanged after bending for 1000 cycles (Fig. 5i).

Considering the wide applicability of CNT and graphene, all-carbon-electrode-based flexible PSCs were fabricated with graphene as transparent anode and cross-stacking aligned CNT films as cathode [15]. The as-fabricated flexible devices with and without 2,2′,7,7′-tetrakis[*N*,*N*-di(4-methoxyphenyl)amino]-9,9′-

spirobifluorene (spiro-OMeTAD) HTL achieved PCEs of 11.9% and 8.4%, respectively. The flexible PSCs also demonstrated superior robustness against mechanical deformation compared with their counterparts fabricated on ITO based flexible anode.

4. Conclusion and perspective

Flexible solar cells including dye-sensitized solar cells, organic solar cells and perovskite solar cells, have gained increasing attentions worldwide. Although great progress has been made continuously, flexible solar cells still suffer from some tough obstacles before industrialization. Here we summarize the challenges and future directions of flexible solar cells especially for those based on carbon nanomaterials.

Typically, flexible solar cells can be classified into planar and fiber shapes. For a planar form, carbon nanomaterials are deposited on polymer films as flexible electrodes. Developing new flexible and thinner polymer film suitable for photovoltaic device processing may be benefit for high flexibility. For another, great efforts can be made to design intrinsic flexible carbon nanomaterials with stable adhesion to the polymer substrate, such as aligning the carbon nanomaterials in a polymer matrix. In the case of emerging important applications such as wearable electronics, fiber-shaped solar cells are developed for better flexibility, and endurable to bending, twisting and even stretching. Fiber-shaped solar cells are often fabricated on thin metal wires. Benefiting from the good flexibility, high conductivity and mechanical strength, carbon nanomaterials based fibers can function as flexible fiber electrodes themselves. Further, highly flexible or stretchable polymer fibers can be modified by carbon nanomaterials as electrodes, which thus endow the solar cells with higher flexibility and stretchability.

Despite of high optical and mechanical properties, the electrical conductivities of carbon nanomaterials assembled in macroscopic scale usually below 10^4 S/cm are not high enough compared with metal electrodes (~10^5 S/cm), thus resulting in solar cells with decreased performances such as low FF and J_{SC}. Actually, the gap among carbon nanomaterials almost account for the total electrical resistance, which increases the contact resistance. Defect is another key reason. The assembling of them into high-quality macroscopic materials with optimized electronic structure is potentially effective for high electrical conductivity. Besides, composite or hybrid materials by combining a conductive second phase with carbon nanomaterial also represents a general and efficient strategy to improve the electrical conductivity.

Easy fabrication and purification of carbon nanomaterials are crucial to achieve high efficiency. High-quality carbon nanomaterials often need vacuum and high temperature fabrication process which causes much energy consumption. Even though ideal carbon nanomaterials are obtained, it is still challenging to deposit them on substrates particularly on polymer substrates, considering the difference and compatibility between the two parts. Whatever depositing/coating techniques are adopted, they share similar prerequisites for commercialization, such as low temperature, low cost and high throughput. In addition, roll-to-roll processing has been anticipated to be most feasible and promising by virtue of in-line mass production on long flexible substrates. Cost-effective solution processing is developed for almost all the layers in solar cells which can reduce energy payback time. Although used in the laboratory-scale cells generally, spin-coating is still far from industry-level production. Spray-coating, dip-coating and blade-coating are attractive alternatives owing to simple processes, and proper precursors are needed to realize efficient coating. It is worth mentioning that those coating techniques are suitable for both planar and fiber-shaped solar cells. Printing techniques in the ambient air such as screen printing and inkjet printing can be used to realize flexible solar cells with easy patterning and design. Slot-die coating is proved efficient in the fabrication of flexible PSCs with high performance, during which the thickness is controllable. Indeed, slot-die coating is appropriate for large-area production thanks to its ease and low maintenance. Non-trivial efforts should be spent to choose or develop suitable manufacturing processes for flexible solar cells based on roll-to-roll production line.

Flexible solar cells based on low-temperature (<150 °C) and solution-processed ETL are usually subjected to performance and stability loss as serious charge recombination occurs. Strategies to address the interfacial problems should arouse wide attention. A contact-passivation method can be adopted to reduce interfacial recombination and enhance interface binding by using interfacial chlorine atoms on the TiO_2 colloidal nanocrystals to suppress deep trap states at the TiO_2/perovskite interface. Although the successful case is just available for the PSCs on the rigid substrate, it offers a promising strategy to deal with the interfacial problems for flexible solar cells too. The morphology and composition of photoactive layer are also important to device efficiency. Considering the polymer substrates different from rigid ones, changing the precursor ratio of perovskite proves helpful for a high-quality perovskite photoactive film. Besides, compared with flexible solar cells based on polymer substrates, metal substrates especially metal wires are effective electrodes for bearing high processing temperature and realizing good flexibility simultaneously.

Not just high PCE, but long time operational stability is critical as well when assessing the industrial feasibility of a solar cell. Considering the intrinsic vulnerability to external factors of polymer substrates, it is more challenging to encapsulate flexible solar cells. Improved stability can be achieved via effective encapsulation. For flexible fiber-shaped solar cells, encapsulation is more troublesome due to the one-dimensional structure. Besides the operational stability, mechanical stability is also important given various deformations of flexible solar cells during use. To ensure mechanical stability, appropriate manufacturing processes for compact deposition/coating and robust flexible electrode materials are key points to avoid material displacement and device decay.

Even if the above problems are solved, there remain some important issues to be addressed, e.g., maximizing the usage of light to generate electricity. Materials with different band gaps correspond to different absorption wavelength ranges. Therefore, high-performance tandem solar cells are attractive solutions to realize broader sunlight harvesting, e.g., flexible polymer tandem solar cells. Considering the intermittent nature, power generated by flexible solar cells in the daytime needs to be stored. Thus, integrated system is suggested to combine the flexible solar cells with flexible energy storage devices such as batteries and electrochemical capacitors. Last but not least, it is significant to realize electricity generation under ambient lighting, which can get rid of the limitation of weather and time. To this end, DSCs show greater potentials in operating effectively under ambient lighting than the other photovoltaic technologies, which can facilitate the Internet of Things.

Acknowledgements

This work was supported by MOST (2016YFA0203302), NSFC (21634003, 51573027, 51673043, 21604012, 21503079), STCSM (16JC1400702, 17QA1400400, 18QA1400700, 18QA1400800, 15JC1490200) and SHMEC (2017-01-07-00-07-E00062).

References

[1] Y. Li, L. Meng, Y.M. Yang, G. Xu, Z. Hong, Q. Chen, et al., High-efficiency robust

perovskite solar cells on ultrathin flexible substrates, Nat. Commun. 7 (2016) 10214.
[2] J. Chen, Y. Huang, N. Zhang, H. Zou, R. Liu, C. Tao, et al., Micro-cable structured textile for simultaneously harvesting solar and mechanical energy, Nat. Energy 1 (10) (2016) 16138.
[3] K. Zhang, K. Gao, R. Xia, Z. Wu, C. Sun, J. Cao, et al., High-performance polymer tandem solar cells employing a new n-type conjugated polymer as an interconnecting layer, Adv. Mater. 28 (24) (2016) 4817–4823.
[4] S. Jung, J. Lee, J. Seo, U. Kim, Y. Choi, H. Park, Development of annealing-free, solution-processable inverted organic solar cells with N-Doped graphene electrodes using zinc oxide nanoparticles, Nano Lett. 18 (2) (2018) 1337–1343.
[5] L. Qiu, J. Deng, X. Lu, Z. Yang, H. Peng, Integrating perovskite solar cells into a flexible fiber, Angew. Chem. Int. Ed. 53 (39) (2014) 10425–10428.
[6] M. Kaltenbrunner, G. Adam, E.D. Glowacki, M. Drack, R. Schwödiauer, L. Leonat, et al., Flexible high power-per-weight perovskite solar cells with chromium oxide-metal contacts for improved stability in air, Nat. Mater. 14 (10) (2015) 1032–1039.
[7] Y. Zhang, Z. Wu, P. Li, L.K. Ono, Y. Qi, J. Zhou, et al., Fully solution-processed tco-free semitransparent perovskite solar cells for tandem and flexible applications, Adv. Energy Mater 8 (1) (2018) 1701569.
[8] M.B. Schubert, J.H. Werner, Flexible solar cells for clothing, Mater. Today 9 (6) (2006) 42–50.
[9] F. Bonaccorso, L. Colombo, G. Yu, M. Stoller, V. Tozzini, A.C. Ferrari, et al., Graphene, related two-dimensional crystals, and hybrid systems for energy conversion and storage, Science 347 (6217) (2015) 1246501.
[10] P. Cheng, X. Zhan, Stability of organic solar cells: challenges and strategies, Chem. Soc. Rev. 45 (9) (2016) 2544–2582.
[11] A. Abate, J.P. Correa-Baena, M. Saliba, M.S. Su'ait, F. Bella, Perovskite Solar Cells: From the Laboratory to the Assembly Line, Chem.-Eur. J 24 (13) (2018) 3083–3100.
[12] A. Polman, M. Knight, E.C. Garnett, B. Ehrler, W.C. Sinke, Photovoltaic materials: present efficiencies and future challenges, Science (6283) (2016) 352, aad4424.
[13] H. Tan, A. Jain, O. Voznyy, X. Lan, F. de Arquer, J. Fan, et al., Efficient and stable solution-processed planar perovskite solar cells via contact passivation, Science 355 (6326) (2017) 722–726.
[14] C. Bi, B. Chen, H. Wei, S. DeLuca, J. Huang, Efficient flexible solar cell based on composition-tailored hybrid perovskite, Adv. Mater. 29 (30) (2017) 1605900.
[15] Q. Luo, H. Ma, Q. Hou, Y. Li, J. Ren, X. Dai, et al., All-carbon-electrode-based endurable flexible perovskite solar cells, Adv. Funct. Mater. 28 (11) (2018) 1706777.
[16] X. Zhang, K. Aitola, C. Hägglund, A. Kaskela, M.B. Johansson, K. Sveinbjörnsson, et al., Dry-deposited transparent carbon nanotube film as front electrode in colloidal quantum dot solar cells, ChemSusChem 10 (2) (2017) 434–441.
[17] P. Chen, Y. Xu, S. He, X. Sun, S. Pan, J. Deng, et al., Hierarchically arranged helical fibre actuators driven by solvents and vapours, Nat. Nanotechnol. 10 (12) (2015) 1077–1083.
[18] J. Ren, Y. Zhang, W. Bai, X. Chen, Z. Zhang, X. Fang, et al., Elastic and wearable wire-shaped lithium-ion battery with high electrochemical performance, Angew. Chem. Int. Ed. 53 (30) (2014) 7864–7869.
[19] Y. Zhang, W. Bai, X. Cheng, J. Ren, W. Weng, P. Chen, et al., Flexible and stretchable lithium-ion batteries and supercapacitors based on electrically conducting carbon nanotube fiber springs, Angew. Chem. Int. Ed. 53 (52) (2014) 14564–14568.
[20] T. Ye, S.-L. Lim, X. Li, M. Petrović, X. Wang, C. Jiang, et al., Pinhole-free mixed perovskite film for bending durable mixed perovskite solar cells, Sol. Energy Mater. Sol. Cells 175 (2018) 111–117.
[21] Z. Zhang, L. Wei, X. Qin, Y. Li, Carbon nanomaterials for photovoltaic process, Nano Energy 15 (2015) 490–522.
[22] B. O'regan, M. Grätzel, A low-cost, high-efficiency solar cell based on dye-sensitized colloidal TiO_2 films, Nature 353 (6346) (1991) 737–740.
[23] M. Freitag, J. Teuscher, Y. Saygili, X. Zhang, F. Giordano, P. Liska, et al., Dye-sensitized solar cells for efficient power generation under ambient lighting, Nat. Photonics 11 (6) (2017) 372–378.
[24] N. Zhang, J. Chen, Y. Huang, W. Guo, J. Yang, J. Du, et al., A wearable all-solid photovoltaic textile, Adv. Mater. 28 (2) (2016) 263–269.
[25] L. Song, Y. Guan, P. Du, Y. Yang, F. Ko, J. Xiong, Enhanced efficiency in flexible dye-sensitized solar cells by a novel bilayer photoanode made of carbon nanotubes incorporated TiO_2 nanorods and branched TiO_2 nanotubes, Sol. Energy Mater. Sol. Cells 147 (2016) 134–143.
[26] F. Bella, A. Lamberti, S. Bianco, E. Tresso, C. Gerbaldi, C.F. Pirri, Floating, flexible polymeric dye-sensitized solar-cell architecture: the way of near-future photovoltaics, Adv. Mater. Technol 1 (2) (2016) 1600002.
[27] M. Ye, X. Wen, M. Wang, J. Iocozzia, N. Zhang, C. Lin, et al., Recent advances in dye-sensitized solar cells: from photoanodes, sensitizers and electrolytes to counter electrodes, Mater. Today 18 (3) (2015) 155–162.
[28] N. Gasparini, L. Lucera, M. Salvador, M. Prosa, G.D. Spyropoulos, P. Kubis, et al., High-performance ternary organic solar cells with thick active layer exceeding 11% efficiency, Energy Environ. Sci. 10 (4) (2017) 885–892.
[29] D. Angmo, J. Sweelssen, R. Andriessen, Y. Galagan, F.C. Krebs, Inkjet printing of back electrodes for inverted polymer solar cells, Adv. Energy Mater 3 (9) (2013) 1230–1237.
[30] Y. Li, G. Xu, C. Cui, Y. Li, Flexible and semitransparent organic solar cells, Adv. Energy Mater 8 (7) (2018) 1701791.
[31] W. Yang, B. Park, E. Jung, N. Jeon, Y. Kim, D. Lee, Iodide management in formamidinium-lead-halide-based perovskite layers for efficient solar cells, Science 356 (6345) (2017) 1376–1379.
[32] C. Roldán-Carmona, O. Malinkiewicz, A. Soriano, G. Mínguez Espallargas, A. Garcia, P. Reinecke, et al., Flexible high efficiency perovskite solar cells, Energy Environ. Sci. 7 (3) (2014) 994–997.
[33] H. Zhang, J. Cheng, F. Lin, H. He, J. Mao, K.S. Wong, et al., Pinhole-free and surface-nanostructured NiOX film by room-temperature solution process for high-performance flexible perovskite solar cells with good stability and reproducibility, ACS Nano 10 (1) (2016) 1503–1511.
[34] F. Di Giacomo, A. Fakharuddin, R. Jose, T.M. Brown, Progress, challenges and perspectives in flexible perovskite solar cells, Energy Environ. Sci. 9 (10) (2016) 3007–3035.
[35] D. Wang, M. Wright, N.K. Elumalai, A. Uddin, Stability of perovskite solar cells, Sol. Energy Mater. Sol. Cells 147 (2016) 255–275.
[36] K. Rana, J. Singh, J.-H. Ahn, A graphene-based transparent electrode for use in flexible optoelectronic devices, J. Mater. Chem. C 2 (15) (2014) 2646–2656.
[37] X. Yin, P. Chen, M. Que, Y. Xing, W. Que, C. Niu, et al., Highly efficient flexible perovskite solar cells using solution-derived NiO_X hole contacts, ACS Nano 10 (3) (2016) 3630–3636.
[38] I. Jeon, T. Chiba, C. Delacou, Y. Guo, A. Kaskela, O. Reynaud, et al., Single-walled carbon nanotube film as electrode in indium-free planar heterojunction perovskite solar cells: investigation of electron-blocking layers and dopants, Nano Lett. 15 (10) (2015) 6665–6671.
[39] Z. Yin, J. Zhu, Q. He, X. Cao, C. Tan, H. Chen, et al., Graphene-based materials for solar cell applications, Adv. Energy Mater 4 (1) (2014) 1300574.
[40] J.M. Macak, H. Tsuchiya, A. Ghicov, K. Yasuda, R. Hahn, S. Bauer, et al., TiO_2 nanotubes: self-organized electrochemical formation, properties and applications, Curr. Opin. Solid State Mater. Sci. 11 (1–2) (2007) 3–18.
[41] T. Chen, L. Qiu, Z. Cai, F. Gong, Z. Yang, Z. Wang, et al., Intertwined aligned carbon nanotube fiber based dye-sensitized solar cells, Nano Lett. 12 (5) (2012) 2568–2572.
[42] J. You, Z. Hong, Y. Yang, Q. Chen, M. Cai, T.-B. Song, et al., Low-temperature solution-processed perovskite solar cells with high efficiency and flexibility, ACS Nano 8 (2) (2014) 1674–1680.
[43] Z. Chen, G. Yang, X. Zheng, H. Lei, C. Chen, J. Ma, et al., Bulk heterojunction perovskite solar cells based on room temperature deposited hole-blocking layer: suppressed hysteresis and flexible photovoltaic application, J. Power Sources 351 (2017) 123–129.
[44] J. Troughton, D. Bryant, K. Wojciechowski, M.J. Carnie, H. Snaith, D.A. Worsley, et al., Highly efficient, flexible, indium-free perovskite solar cells employing metallic substrates, J. Mater. Chem. 3 (17) (2015) 9141–9145.
[45] X. Wang, Z. Li, W. Xu, S.A. Kulkarni, S.K. Batabyal, S. Zhang, et al., TiO_2 nanotube arrays based flexible perovskite solar cells with transparent carbon nanotube electrode, Nano Energy 11 (2015) 728–735.
[46] G. Liu, H. Wang, M. Wang, W. Liu, R.E. Anugrah Ardhi, D. Zou, et al., Study on a stretchable, fiber-shaped, and TiO_2 nanowire array-based dye-sensitized solar cell with electrochemical impedance spectroscopy method, Electrochim. Acta 267 (2018) 34–40.
[47] Y. Fu, Z. Lv, S. Hou, H. Wu, D. Wang, C. Zhang, et al., Conjunction of fiber solar cells with groovy micro-reflectors as highly efficient energy harvesters, Energy Environ. Sci. 4 (9) (2011) 3379–3383.
[48] H. Sun, X. You, J. Deng, X. Chen, Z. Yang, P. Chen, et al., A twisted wire-shaped dual-function energy device for photoelectric conversion and electrochemical storage, Angew. Chem. Int. Ed. 53 (26) (2014) 6664–6668.
[49] H. Sun, X. You, J. Deng, X. Chen, Z. Yang, J. Ren, et al., Novel graphene/carbon nanotube composite fibers for efficient wire-shaped miniature energy devices, Adv. Mater. 26 (18) (2014) 2868–2873.
[50] H. Kroto, J. Heath, S. O'Brien, R. Curl, R. Smalley, C60: buckminsterfullerene, Nature 318 (6042) (1985) 162–163.
[51] R. Ganesamoorthy, G. Sathiyan, P. Sakthivel, Review: fullerene based acceptors for efficient bulk heterojunction organic solar cell applications, Sol. Energy Mater. Sol. Cells 161 (2017) 102–148.
[52] G. Yu, J. Gao, J.C. Hummelen, F. Wudl, A.J. Heeger, Polymer photovoltaic cells: enhanced efficiencies via a network of internal donor-acceptor heterojunctions, Science 270 (5243) (1995) 1789–1791.
[53] C. Cui, Y. Li, Y. Li, Fullerene derivatives for the applications as acceptor and cathode buffer layer materials for organic and perovskite solar cells, Adv. Energy Mater 7 (10) (2017) 1601251.
[54] M.M. Wienk, J.M. Kroon, W.J. Verhees, J. Knol, J.C. Hummelen, P.A. van Hal, et al., Efficient methano [70] fullerene/MDMO-PPV bulk heterojunction photovoltaic cells, Angew. Chem. Int. Ed. 42 (29) (2003) 3371–3375.
[55] Y. Shao, Y. Yuan, J. Huang, Correlation of energy disorder and open-circuit voltage in hybrid perovskite solar cells, Nat. Energy 1 (1) (2016) 15001.
[56] S. Iijima, Helical microtubules of graphitic carbon, Nature 354 (6348) (1991) 56–58.
[57] L. Yu, C. Shearer, J. Shapter, Recent development of carbon nanotube transparent conductive films, Chem. Rev. 116 (22) (2016) 13413–13453.
[58] D. Mann, A. Javey, J. Kong, Q. Wang, H. Dai, Ballistic transport in metallic nanotubes with reliable Pd ohmic contacts, Nano Lett. 3 (11) (2003) 1541–1544.
[59] G. Chen, D.N. Futaba, S. Sakurai, M. Yumura, K. Hata, Interplay of wall number and diameter on the electrical conductivity of carbon nanotube thin films,

Carbon 67 (2014) 318–325.
[60] M. in het Panhuis, Carbon nanotubes: enhancing the polymer building blocks for intelligent materials, J. Mater. Chem. 16 (36) (2006) 3598–3605.
[61] P. Zhou, X. Yang, L. He, Z. Hao, W. Luo, B. Xiong, et al., The Young's modulus of high-aspect-ratio carbon/carbon nanotube composite microcantilevers by experimental and modeling validation, Appl. Phys. Lett. 106 (11) (2015) 111908.
[62] M. Cinke, J. Li, B. Chen, A. Cassell, L. Delzeit, J. Han, et al., Pore structure of raw and purified HiPco single-walled carbon nanotubes, Chem. Phys. Lett. 365 (1–2) (2002) 69–74.
[63] P. Kim, L. Shi, A. Majumdar, P.L. McEuen, Thermal transport measurements of individual multiwalled nanotubes, Phys. Rev. Lett. 87 (21) (2001) 215502.
[64] K. Novoselov, A. Geim, S. Morozov, D. Jiang, Y. Zhang, S. Dubonos, et al., Electric field effect in atomically thin carbon films, Science 306 (5696) (2004) 666–669.
[65] J.-H. Chen, C. Jang, S. Xiao, M. Ishigami, M.S. Fuhrer, Intrinsic and extrinsic performance limits of graphene devices on SiO_2, Nat. Nanotechnol. 3 (4) (2008) 206–209.
[66] T. Ohta, A. Bostwick, T. Seyller, K. Horn, E. Rotenberg, Controlling the electronic structure of bilayer graphene, Science 313 (5789) (2006) 951–954.
[67] A.A. Balandin, S. Ghosh, W. Bao, I. Calizo, D. Teweldebrhan, F. Miao, et al., Superior thermal conductivity of single-layer graphene, Nano Lett. 8 (3) (2008) 902–907.
[68] G.S. Selopal, R. Milan, L. Ortolani, V. Morandi, R. Rizzoli, G. Sberveglieri, et al., Graphene as transparent front contact for dye sensitized solar cells, Sol. Energy Mater. Sol. Cells 135 (2015) 99–105.
[69] J.D. Roy-Mayhew, I.A. Aksay, Graphene materials and their use in dye-sensitized solar cells, Chem. Rev. 114 (12) (2014) 6323–6348.
[70] S. Pan, Z. Yang, H. Li, L. Qiu, H. Sun, H. Peng, Efficient dye-sensitized photovoltaic wires based on an organic redox electrolyte, J. Am. Chem. Soc. 135 (29) (2013) 10622–10625.
[71] A. Ali, K. Shehzad, F. Ur-Rahman, S.M. Shah, M. Khurram, M. Mumtaz, et al., Flexible, low cost, and platinum-free counter electrode for efficient dye-sensitized solar cells, ACS Appl. Mater. Interfaces 8 (38) (2016) 25353–25360.
[72] Y. Jiang, H. Sun, H. Peng, Synthesis and photovoltaic application of platinum-modified conducting aligned nanotube fiber, Sci. China Mater 58 (4) (2015) 289–293.
[73] S. He, P. Chen, L. Qiu, B. Wang, X. Sun, Y. Xu, et al., A mechanically actuating carbon-nanotube fiber in response to water and moisture, Angew. Chem. Int. Ed. 54 (49) (2015) 14880–14884.
[74] X. Fu, H. Sun, S. Xie, J. Zhang, Z. Pan, M. Liao, et al., A fiber-shaped solar cell showing a record power conversion efficiency of 10%, J. Mater. Chem. 6 (1) (2018) 45–51.
[75] Z. Yang, J. Deng, X. Sun, H. Li, H. Peng, Stretchable, wearable dye-sensitized solar cells, Adv. Mater. 26 (17) (2014) 2643–2647.
[76] T. Chen, S. Wang, Z. Yang, Q. Feng, X. Sun, L. Li, et al., Flexible, light-weight, ultrastrong, and semiconductive carbon nanotube fibers for a highly efficient solar cell, Angew. Chem. Int. Ed. 50 (8) (2011) 1815–1819.
[77] J. Lee, H. Kang, J.-Y. Hwang, S.W. Kim, S. Baik, Flexible photoanodes of TiO_2 particles and metallic single-walled carbon nanotubes for flexible dye-sensitized solar cells, Carbon 79 (2014) 337–345.
[78] I.A. Sahito, K.C. Sun, A.A. Arbab, M.B. Qadir, Y.S. Choi, S.H. Jeong, Flexible and conductive cotton fabric counter electrode coated with graphene nanosheets for high efficiency dye sensitized solar cell, J. Power Sources 319 (2016) 90–98.
[79] I.-Y. Jeon, H.M. Kim, I.T. Choi, K. Lim, J. Ko, J.C. Kim, et al., High-performance dye-sensitized solar cells using edge-halogenated graphene nanoplatelets as counter electrodes, Nano Energy 13 (2015) 336–345.
[80] L. Sun, L. Lu, Y. Bai, K. Sun, Three-dimensional porous reduced graphene oxide/sphere-like CoS hierarchical architecture composite as efficient counter electrodes for dye-sensitized solar cells, J. Alloy. Comp. 654 (2016) 196–201.
[81] Y. Peng, J. Zhong, K. Wang, B. Xue, Y.-B. Cheng, A printable graphene enhanced composite counter electrode for flexible dye-sensitized solar cells, Nano Energy 2 (2) (2013) 235–240.
[82] Z. Yang, H. Sun, T. Chen, L. Qiu, Y. Luo, H. Peng, Photovoltaic wire derived from a graphene composite fiber achieving an 8.45% energy conversion efficiency, Angew. Chem. Int. Ed. 52 (29) (2013) 7545–7548.
[83] J. Zhi, H. Cui, A. Chen, Y. Xie, F. Huang, Efficient highly flexible dye sensitized solar cells of three dimensional graphene decorated titanium dioxide nanoparticles on plastic substrate, J. Power Sources 281 (2015) 404–410.
[84] Z. Yu, L. Li, Q. Zhang, W. Hu, Q. Pei, Silver nanowire-polymer composite electrodes for efficient polymer solar cells, Adv. Mater. 23 (38) (2011) 4453–4457.
[85] L. La Notte, P. Cataldi, L. Ceseracciu, I.S. Bayer, A. Athanassiou, S. Marras, et al., Fully-sprayed flexible polymer solar cells with a cellulose-graphene electrode, Mater. Today Energy 7 (2018) 105–112.
[86] J. Zhang, R. Xue, G. Xu, W. Chen, G.-Q. Bian, C. Wei, et al., Self-doping fullerene electrolyte-based electron transport layer for all-room-temperature-processed high-performance flexible polymer solar cells, Adv. Funct. Mater. 28 (13) (2018) 1705847.
[87] I. Jeon, K. Cui, T. Chiba, A. Anisimov, A.G. Nasibulin, E.I. Kauppinen, et al., Direct and dry deposited single-walled carbon nanotube films doped with MoO(x) as electron-blocking transparent electrodes for flexible organic solar cells, J. Am. Chem. Soc. 137 (25) (2015) 7982–7985.
[88] I. Jeon, C. Delacou, A. Kaskela, E.I. Kauppinen, S. Maruyama, Y. Matsuo, Metal-electrode-free window-like organic solar cells with p-doped carbon nanotube thin-film electrodes, Sci. Rep. 6 (2016) 31348.
[89] R.V. Salvatierra, C.E. Cava, L.S. Roman, A.J. Zarbin, ITO-free and flexible organic photovoltaic device based on high transparent and conductive polyaniline/carbon nanotube thin films, Adv. Funct. Mater. 23 (12) (2013) 1490–1499.
[90] S. Ren, M. Bernardi, R.R. Lunt, V. Bulovic, J.C. Grossman, S. Gradečak, Toward efficient carbon nanotube/P3HT solar cells: active layer morphology, electrical, and optical properties, Nano Lett. 11 (12) (2011) 5316–5321.
[91] Z. Zhang, Z. Yang, Z. Wu, G. Guan, S. Pan, Y. Zhang, et al., Weaving efficient polymer solar cell wires into flexible power textiles, Adv. Energy Mater 4 (11) (2014) 1301750.
[92] Z. Zhang, Z. Yang, J. Deng, Y. Zhang, G. Guan, H. Peng, Stretchable polymer solar cell fibers, Small 11 (6) (2015) 675–680.
[93] H. Park, S. Chang, X. Zhou, J. Kong, T. Palacios, S. Gradečak, . Flexible graphene electrode-based organic photovoltaics with record-high efficiency, Nano Lett. 14 (9) (2014) 5148–5154.
[94] Y. Song, S. Chang, S. Gradečak, J. Kong, Visibly-transparent organic solar cells on flexible substrates with all-graphene electrodes, Adv. Energy Mater 6 (20) (2016) 1600847.
[95] D.H. Shin, C.W. Jang, H.S. Lee, S.W. Seo, S.H. Choi, Semitransparent flexible organic solar cells employing doped-graphene layers as anode and cathode electrodes, ACS Appl. Mater. Interfaces 10 (4) (2018) 3596–3601.
[96] P. Docampo, J.M. Ball, M. Darwich, G.E. Eperon, H.J. Snaith, Efficient organometal trihalide perovskite planar-heterojunction solar cells on flexible polymer substrates, Nat. Commun. 4 (2013) 2761.
[97] J.H. Heo, M. Jahandar, S.-J. Moon, C.E. Song, S.H. Im, Inverted $CH_3NH_3PbI_3$ perovskite hybrid solar cells with improved flexibility by introducing a polymeric electron conductor, J. Mater. Chem. C 5 (11) (2017) 2883–2891.
[98] H. Lei, X. Chen, L. Xue, L. Sun, J. Chen, Z. Tan, et al., A solution-processed pillar [5] arene-based small molecule cathode buffer layer for efficient planar perovskite solar cells, Nanoscale 10 (17) (2018) 8088–8098.
[99] U. Ryu, S. Jee, J.-S. Park, I.K. Han, J.H. Lee, M. Park, et al., Nanocrystalline titanium metal–organic frameworks for highly efficient and flexible perovskite solar cells, ACS Nano 12 (5) (2018) 4968–4975.
[100] Y.-Q. Zhou, B.-S. Wu, G.-H. Lin, Y. Li, D.-C. Chen, P. Zhang, et al., Enhancing performance and uniformity of perovskite solar cells via a solution-processed C70 interlayer for interface engineering, ACS Appl. Mater. Interfaces 9 (39) (2017) 33810–33818.
[101] J. Deng, L. Qiu, X. Lu, Z. Yang, G. Guan, Z. Zhang, et al., Elastic perovskite solar cells, J. Mater. Chem. 3 (42) (2015), 21070-21076.
[102] L. Qiu, S. He, J. Yang, F. Jin, J. Deng, H. Sun, et al., An all-solid-state fiber-type solar cell achieving 9.49% efficiency, J. Mater. Chem. 4 (26) (2016) 10105–10109.
[103] Z. Liu, P. You, C. Xie, G. Tang, F. Yan, Ultrathin and flexible perovskite solar cells with graphene transparent electrodes, Nano Energy 28 (2016) 151–157.
[104] I. Jeon, J. Yoon, N. Ahn, M. Atwa, C. Delacou, A. Anisimov, et al., Carbon nanotubes versus graphene as flexible transparent electrodes in inverted perovskite solar cells, J. Phys. Chem. Lett. 8 (21) (2017) 5395–5401.
[105] J. Yoon, H. Sung, G. Lee, W. Cho, N. Ahn, H.S. Jung, et al., Superflexible, high-efficiency perovskite solar cells utilizing graphene electrodes: towards future foldable power sources, Energy Environ. Sci. 10 (1) (2017) 337–345.